Biochemical and Biophysical Research Communications 456 (2015) 13–19

Contents lists available at ScienceDirect

Biochemical and Biophysical Research Communications

journal homepage: www.elsevier.com/locate/ybbrc

Longitudinal monitoring adipose-derived stem cell survival by PET imaging hexadecyl-4-^{124}I-iodobenzoate in rat myocardial infarction model

Min Hwan Kim [a,b], Sang-Keun Woo [a], Kyo Chul Lee [a], Gwang Il An [a], Darpan Pandya [c], Noh Won Park [d], Sang-Soep Nahm [d], Ki Dong Eom [d], Kwang Il Kim [a], Tae Sup Lee [a], Chan Wha Kim [b], Joo Hyun Kang [a], Jeongsoo Yoo [c,*], Yong Jin Lee [a,*]

[a] Molecular Imaging Research Center, Korea Institute of Radiological and Medical Sciences, Seoul, Republic of Korea
[b] School of Life Sciences and Biotechnology, Korea University, Seoul, Republic of Korea
[c] Department of Molecular Medicine, BK21 Plus KNU Biomedical Convergence Program, Kyungpook National University, Daegu, Republic of Korea
[d] College of Veterinary Medicine, Konkuk University, Seoul, Republic of Korea

ARTICLE INFO

Article history:
Received 3 November 2014
Available online 15 November 2014

Keywords:
Adipose-derived stem cells
Cell tracking
Direct labeling agent
Hexadecyl-4-^{124}I-iodobenzoate
Myocardial infarction

ABSTRACT

This study aims to monitor how the change of cell survival of transplanted adipose-derived stem cells (ADSCs) responds to myocardial infarction (MI) via the hexadecyl-4-^{124}I-iodobenzoate (^{124}I-HIB) mediated direct labeling method in vivo. Stem cells have shown the potential to improve cardiac function after MI. However, monitoring of the fate of transplanted stem cells at target sites is still unclear. Rat ADSCs were labeled with ^{124}I-HIB, and radiolabeled ADSCs were transplanted into the myocardium of normal and MI model. In the group of ^{124}I-HIB-labeled ADSC transplantation, in vivo imaging was performed using small-animal positron emission tomography (PET)/computed tomography (CT) for 9 days. Twenty-one days post-transplantation, histopathological analysis and apoptosis assay were performed. ADSC viability and differentiation were not affected by ^{124}I-HIB labeling. In vivo tracking of the ^{124}I-HIB-labeled ADSCs was possible for 9 and 3 days in normal and MI model, respectively. Apoptosis of transplanted cells increased in the MI model compared than that in normal model. We developed a direct labeling agent, ^{124}I-HIB, and first tried to longitudinally monitor transplanted stem cell to MI. This approach may provide new insights on the roles of stem cell monitoring in living bodies for stem cell therapy from pre-clinical studies to clinical trials.

1. Introduction

Myocardial infarction (MI) occurs when blood supply reduced to a part of heart tissue, and is the leading cause of mortality and morbidity in developed country [1–3]. MI induced loss and necrosis of resident cardiomyocytes, and the injured myocardium replaced with scar tissue by fibrosis to maintain structural rigidity. Stem cell therapy shows promise in patients with heart disease, including in those with acute MI and chronic ischemia. Various types of stem cells can be isolated from different tissues such as bone marrow, skin, amniotic fluid, and adipose tissue [4–8]. In particular, adipose-derived stem cells (ADSCs) have been a focus of study due to their general abundance, easy cell isolation, and ability to proliferate and differentiate [9–11]. Injected ADSCs can be engraft and differentiate into cardiomyocytes and endothelial cells in MI model [9], and ADSCs therapy for MI repair has shown improvement on cardiac function through elevation of angiogenesis via paracrine factor [12], and cardiac remodeling attenuation [13]. To date, numerous studies including preclinical study and clinical trials have demonstrated that transplantation of circulating progenitor cells (CPCs) or mesenchymal stem cells can recover

Abbreviations: ADSCs, adipose-derived stem cells; CT, computed tomography; DMSO, dimethyl sulfoxide; ^{18}F-FDG, 2-^{18}F-fluoro-2-deoxy-D-glucose; ^{18}F-HFB, hexadecyl-4-^{18}F-fluorobenzoate; ^{124}I-HIB, hexadecyl-4-^{124}I-iodobenzoate; HPLC, high performance liquid chromatography; MI, myocardial infarction; PET, positron emission tomography; ^{99m}Tc-HMPAO, ^{99m}Tc-hexamethyl propylene amine oxime; TUNEL, terminal deoxynucleotidyl transferase (TdT)-mediated dUTP nick end labeling.

* Corresponding authors at: Molecular Imaging Research Center, Korea Institute of Radiological and Medical Sciences (KIRAMS), 75 Nowon-gil, Gongneung-Dong, Nowon-Gu, Seoul 139-706, Republic of Korea (Y.J. Lee). Fax: +82 2 970 1341 (Y.J. Lee).

E-mail addresses: yooj@knu.ac.kr (J. Yoo), yjlee@kirams.re.kr (Y.J. Lee).

http://dx.doi.org/10.1016/j.bbrc.2014.11.019
0006-291X/

regional perfusion and improve cardiac function in the myocardial infarction [14–16]. However, the monitoring of the fate of transplanted stem cells at target sites is poorly understood. Although, histological evaluation can provide the information about effect on stem cell therapy, but they cannot monitor longitudinal change for transplanted stem cells. Thus, serial monitoring the fate of transplanted stem cells for cardiac repair is an important part of regenerative medicine.

Positron emission tomography (PET) provides high sensitivity, good spatial resolution, and cell tracking imaging for transplanted stem cells [17]. Therefore, PET can be applied for a noninvasive imaging technique to monitor for longitudinal stem cell tracking.

In this study, we first tried to monitor the fate of the transplanted stem cells with PET using ^{124}I-HIB for 9 days in normal and MI model.

2. Materials and methods

2.1. Cell isolation and characterization

ADSCs were isolated from male Sprague–Dawley (SD) rats (250 ± 10 g, Narabio, Seoul, Korea) euthanized via carbon dioxide (CO_2) inhalation. Visceral fat encasing the stomach and intestine was dissected and minced to 1–3 mm. The isolated tissue was dissociated for 15 min at 37 °C using 0.1% (w/v) collagenase type I (Worthington Biochemical Corp., Lakewood, NJ). The solution was passed through 70 μm nylon mesh, neutralized using Dulbecco's Modified Eagle's Medium (DMEM) (WELGENE Inc., Daegu, Korea) with 10% (v/v) fetal bovine serum (FBS) (JRScientific, Inc., Woodland, CA), and centrifuged at 250×*g* for 5 min. The cell pellet was re-suspended in DMEM (WELGENE Inc.) containing 10% (v/v) FBS (JRScientific, Inc.) and 1% (v/v) penicillin/streptomycin solution. Cultures were maintained in a 37 °C incubator with 5% CO_2, and the medium was changed every 3 days.

Expression of stem cell-specific surface markers using fluorescein isothiocyanate (FITC)-conjugated CD44 (LSBio, Seattle, WA), phycoerythrin (PE)-conjugated CD90, PE-conjugated CD31, and FITC-conjugated CD45 antibodies (eBioscience, Inc., San Diego, CA) was evaluated with a FACSCalibur flow cytometer (BD Bioscience, San Jose, CA). Isotype control antibodies were used as a negative control.

2.2. Radiochemical synthesis and in vitro study

The radioactive cell labeling agent using in this study, hexadecyl-4-tributylstannylbenzoate, is covered by the patent (publication number: WO 2010074532 A2). ^{124}I-NaI was produced at the Korea Institute of Radiological & Medical Sciences (KIRAMS) via 50 MeV cyclotron irradiation. ^{124}I-NaI (20–92 MBq)-added 50 μL 1 N HCl was added to a mixture of hexadecyl-4-tributylstannylbenzoate (50 μg) in 50 μL of ethyl acetate and 50 μL of 3% H_2O_2, respectively. The mixture reacted for 10 min at room temperature (RT), and then the reaction was terminated by adding 100 μL of saturated $NaHSO_3$. The radioactive ^{124}I-HIB was purified through high performance liquid chromatography (HPLC) (Luna C8 column, 5 μm, 4.6 × 50 mm, mobile phase 95% acetonitrile/H_2O, flow rate of 1 mL/min). The collected pure ^{124}I-HIB was completely dried under a vacuum and dissolved in 20% dimethyl sulfoxide (DMSO)/phosphate buffered saline (PBS) solution for subsequent cell labeling studies. The radiolabeling yield and purity were determined with radio-thin layer chromatography (TLC) using a mobile phase of hexane: EtOAC (20:1 v/v) on a silica plate.

A solution of ^{124}I-HIB (6.3–22.2 MBq, 200 μL) in 20% DMSO/PBS or 2-^{18}F-fluoro-2-deoxy-D-glucose (^{18}F-FDG) (37–74 MBq, 200 μL) was added to a suspension of 5 × 10^6 rat ADSCs in 1 mL PBS, and the mixture was incubated at 37 °C for 1 h. After centrifugation (250×*g*, 5 min), the supernatant was removed, and the cells were washed twice with PBS. The radioactive content of the isolated pellet and supernatant was measured to calculate radiolabeling efficiency using a radioisotope calibrator (CRC®-127R; Capintec, Inc., Ramsey, NJ). This procedure was repeated three times to ensure accurate and efficient cell labeling.

Cell viability of ^{124}I-HIB-labeled ADSCs (n = 3) was determined via the trypan blue dye exclusion test. Leakage ratio of ^{124}I-HIB-labeled ADSCs (9.3–18.5 MBq) (n = 3) in culture medium was investigated by checking radioactivity in the supernatant and cell pellets at various times for 24 h in vitro. Also, the release of ^{124}I-HIB (n = 3) from cell death by distilled water (D.W.) treatment was calculated from the radioactivity ratio of the supernatant and cells.

2.3. Differentiation of ^{124}I-HIB-labeled ADSCs

^{124}I-HIB-labeled ADSCs (3.7–4.0 MBq) were differentiated into osteogenic, chondrogenic, and adipogenic lineages using a STEMPRO® Osteogenesis, Chondrogenesis, and Adipogenesis Differentiation Kit (Gibco, Carlsbad, CA). Each differentiation procedure was performed according to the manufacturer's instructions.

After differentiation, the each cell was fixed with 4% paraformaldehyde for 30 min for the staining procedure. Alizarin Red S, Alcian Blue, and Oil Red O staining were used to investigate osteogenic, chondrogenic, and adipogenic differentiation, respectively. Cardiomyogenic differentiation was processed as described by Carvalho et al. [18].

2.4. Reverse transcriptase-polymerase chain reaction (RT-PCR) analysis

Total RNA from cardiomyogenic induced radiolabeled ADSCs and rat heart were extracted using TRI Reagent (Molecular Research Center, Inc., Cincinnati, OH). Five microgram of total RNA were reverse-transcribed using SuperScript III Reverse Transcriptase (Invitrogen, Grand Island, NY) and random hexamers to generate cDNA. GATA binding protein 4 (GATA-4), NK2 transcription factor related locus 5 (Nkx2-5), ventricular myosin light chain type 2 (MLC-2v), alpha-myosin heavy chain (α-MHC) and β-actin expression were analyzed. Primers for RT-PCR were shown in Supplementary Table 1. After a denaturation phase of 5 min at 94 °C, amplification was performed at an annealing temperature of 56–65 °C for 30 s for 30–35 cycles, then elongation performed at 72 °C for 5 min.

2.5. MI induction and cell transplantation

Female SD rats (250 ± 10 g, Narabio) were used, and the animals were anesthetized with 2% isoflurane (Foran, Choongwae Pharma Co., Seoul, Korea), intubated and maintained on a ventilator. The animals underwent left thoracotomy, and a MI was induced by permanent ligation of the left anterior descending coronary artery. Cell transplantation performed by single intramuscularly injection at the myocardium. ^{124}I-HIB-or ^{18}F-FDG-labeled ADSCs were suspended in PBS (5 × 10^6 cells/50 μL) and kept on ice until transplantation. The ^{124}I-HIB-labeled (1.18–1.48 MBq, n = 3) or ^{18}F-FDG-labeled ADSCs (1.18–1.48 MBq, n = 2) were intramuscularly injected to left myocardium of the normal model. The ^{124}I-HIB-labeled (1.18–1.48 MBq, n = 4) or ^{18}F-FDG-labeled ADSCs (1.18–1.48 MBq, n = 2) were transplanted into the left myocardium, at the infarct site.

2.6. In vivo imaging of ^{124}I-HIB- or ^{18}F-FDG-labeled ADSCs

The care, maintenance, and treatment of animals in these studies followed protocols approved by the Institutional Animal Care and Use Committee of KIRAMS.

Transplanted stem cells were monitored in vivo using a small-animal PET/computed tomography (CT) scanner (Inveon™; Siemens Preclinical Solutions, Malvern, PA). Animals were anesthetized with 2% isoflurane (Foran, Choongwae Pharma Co.) during the imaging process. The ^{124}I-HIB- or ^{18}F-FDG-labeled ADSCs-transplanted animal PET imaging was performed for 30 min for 9 or 1 day after stem cell injection, respectively. CT images were acquired at 70 kVp of X-ray voltage with a 400 μA anode current with a 200 ms exposure time for each step. PET emission data were acquired with three spans and 79 ring differences through a 350–650 keV energy window and 3.43 ns timing windows. The ^{124}I-HIB- or ^{18}F-FDG-labeled ADSC uptake was measured during the PET imaging analysis from a region of interest (ROI) in the target region. All data are expressed as mean ± standard deviation (SD) with decay corrected radioactivity concentration ROI value.

2.7. Histopathological and apoptosis analysis

Rats were sacrificed and myocardial tissue was obtained at 21 days after MI. Rat myocardium transplanted with ^{124}I-HIB-labeled ADSCs was fixed with 4% paraformaldehyde for 24–48 h. The tissue was embedded in paraffin, and 4 μm sections were deparaffinized and rehydrated for staining. Hematoxyin and eosin (H&E) staining, Masson's Trichrome (MT) (Dako, Carpinteria, CA), and terminal transferase dUTP nick end labeling (TUNEL) staining was performed using an ApopTag® Peroxidase *In Situ* Apoptosis Detection Kit (Millipore, Billerica, MA) according to the manufacturer's instructions. Stained tissues were examined with an Olympus IX51 inverted microscope (Olympus). The apoptotic index was determined at ×200 magnification as the proportion

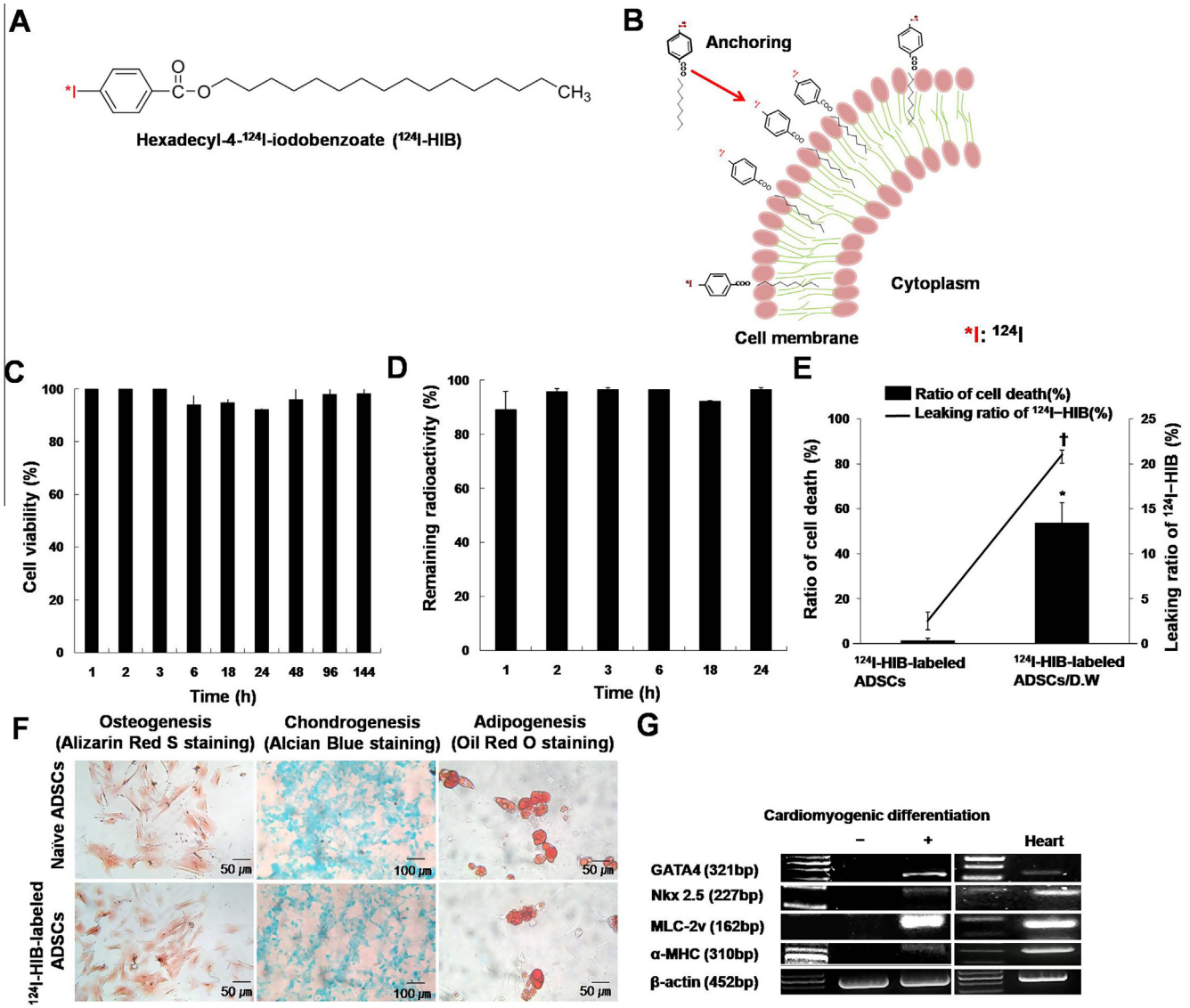

Fig. 1. In vitro characterization and differentiation potential of radiolabeled ADSCs. (A) Chemical structure of ^{124}I-HIB. (B) Schematic diagram of a ^{124}I-HIB-labeled cell. (C) Cell viability of ^{124}I-HIB-labeled ADSCs for 144 h. (D) Remaining radioactivity of ^{124}I-HIB-labeled ADSCs for 24 h. (E) Ratio of dead cells and leaking ^{124}I-HIB from D.W. treated ADSCs (ratio of cell death; $^{*}P < 0.05$ vs. ^{124}I-HIB-labeled ADSCs in PBS, leaking ratio of ^{124}I-HIB; $^{\dagger}P < 0.05$ vs. ^{124}I-HIB-labeled ADSCs in PBS). (F) Alizarin Red S (magnification ×200), Alcian Blue (magnification ×100), and Oil Red O (magnification ×200) staining of lineage-specific differentiated naïve, and ^{124}I-HIB-labeled ADSCs. (G) Cardiac-specific mRNA expression of cardiomyogenic differentiated ^{124}I-HIB-labeled ADSCs.

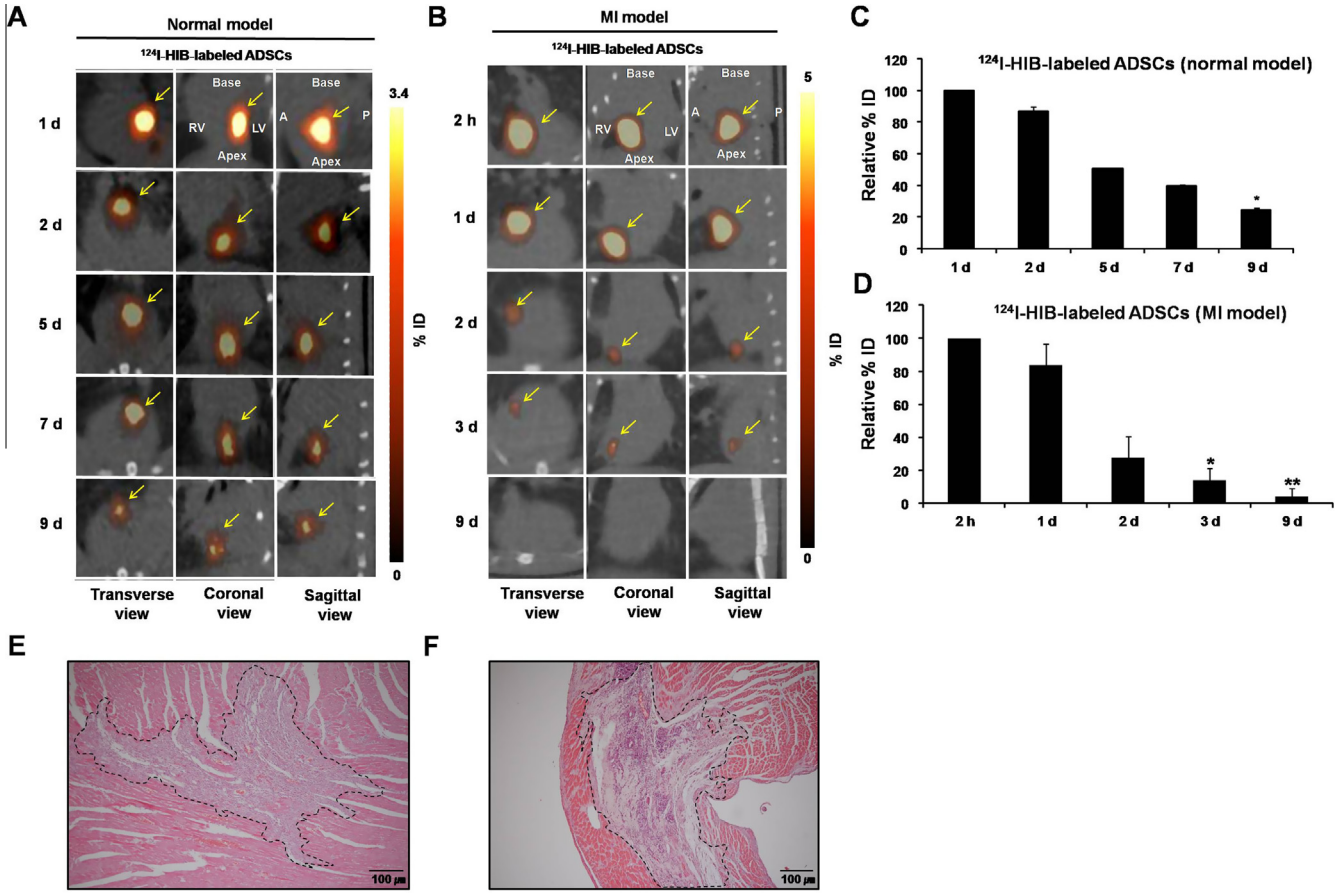

Fig. 2. Small-animal PET/CT imaging of transplanted ^{124}I-HIB-labeled ADSCs in normal and MI model, and longitudinal quantification of the relative percent of injected dose (%ID). (A and B) Small-animal PET/CT images of transplanted ^{124}I-HIB-labeled ADSCs in normal (A) and MI model (B) for 9 days. (C and D) Longitudinal quantification of the relative %ID of transplanted ^{124}I-HIB-labeled ADSCs in normal (C, $^{*}P < 0.05$ vs. day 1) and MI model (D, $^{*}P < 0.05$, $^{**}P < 0.001$ vs. 2 h) for 9 days. (E and F) H&E staining of heart tissues from normal (E) and MI model (F). Dotted line indicated the presumptive site of ADSC injection (magnification ×100). Arrows indicate the inject site of ^{124}I-HIB-labeled ADSCs. A = anterior, P = posterior, RV = right ventricle, LV = left ventricle.

of TUNEL-positive cells relative to the minimal total of 1000 cells in 10 fields. Data are expressed as mean ± SD.

2.8. Statistical analysis

All the data were analyzed using statistical software (SPSS® for windows version 19.0, SPSS Inc., Chicago, IL). One-sample *t*-test was performed to compare mean differences within group, and differences among groups were assessed using one-way analysis of variance. All statistical analyses were considered as significant if $P < 0.05$.

3. Results

3.1. Radiochemical synthesis of ^{124}I-HIB and characterization of ^{124}I-HIB-labeled ADSCs

^{124}I-HIB was prepared with a radiolabeling yield of 97.59 ± 0.43%. Radiochemical purity of ^{124}I-HIB was 92.36 ± 0.28%. The chemical structure of ^{124}I-HIB and cell labeling diagram are shown in Fig. 1. Cell labeling efficiency of ^{124}I-HIB was 51.26 ± 1.20% ($n = 3$), which was 1.8-fold higher than that of ^{18}F-FDG (28.50 ± 10.8%) ($n = 3$, $P < 0.05$). After 144 h of ^{124}I-HIB-labeling, cell viability was 98.21 ± 2.07% ($n = 3$) (Fig. 1C). The remaining ^{124}I-HIB radioactivity of ADSCs was 96.54 ± 0.59% at 24 h ($n = 3$) (Fig. 1D). In the ^{124}I-HIB-labeled ADSCs in PBS, ratio of dead cells was 1.45 ± 0.92% and leaking ratio of ^{124}I-HIB from ADSCs was 2.52 ± 1.02%. Following distilled water (D.W.) treatment, the ratio of dead cells increased by 53.74 ± 8.97% ($P < 0.05$), and the leaking ratio of ^{124}I-HIB from ADSCs increased by 21.05 ± 0.45%, compared to ^{124}I-HIB-labeled ADSCs in PBS (Fig. 1E).

3.2. The phenotype of ADSCs

The adherent cells began to proliferate rapidly and grew into spindle shaped cells (Supplementary Fig. 1A). Also, the ADSCs highly expressed stem cell related markers such as CD44 (47.95%) and CD90 (94.04%) but were nearly negative for expression of endothelial and hematopoietic markers such as CD31 (0.32%) and CD45 (0.30%) (Supplementary Fig. 1B).

3.3. Differentiation of ^{124}I-HIB-labeled ADSCs

The appearance of ADSCs changed from an elongated fibroblastic shape to a round, polygonal configuration in the osteogenic medium. Larger mineralized nodules were formed and stained intensely red with Alizarin Red S 21 days after osteogenic induction. The ADSCs formed cellular spheres and proteoglycan deposits when stained with Alcian Blue 14 days after chondrogenic induction via micro-mass culture. The number of cells filled with lipid droplets increased, and these lipid droplets were stained intensely red with Oil Red O on day 14 of adipogenic induction (Fig. 1F). Fig. 1G showed that cardiomyogenic differentiated ^{124}I-HIB-labeled ADSCs expressed several cardiac-specific transcription factors such as GATA-4 and Nkx2.5 as well as MLC-2v and α-MHC, respectively.

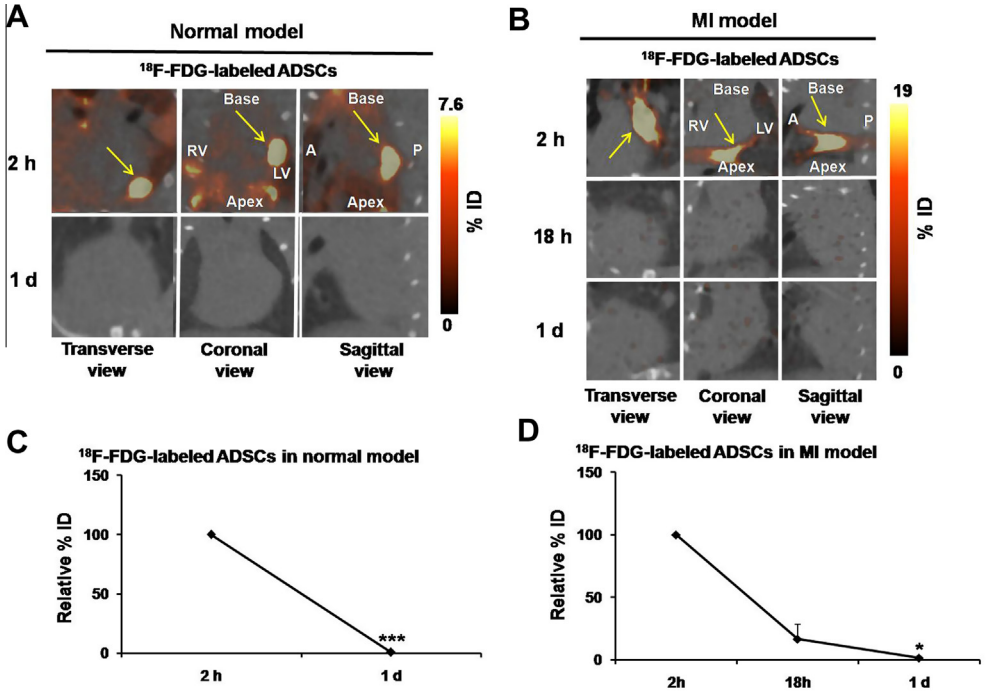

Fig. 3. Small-animal PET/CT imaging of transplanted ^{18}F-FDG-labeled ADSCs in normal and MI model, and longitudinal quantification of relative % ID. (A and B) Small-animal PET/CT images of transplanted ^{18}F-FDG-labeled ADSCs in normal (A) and MI model (B) for 1 day. (C and D) Longitudinal quantification of relative %ID of transplanted ^{18}F-FDG-labeled ADSCs in normal (C, $^{***}P < 0.0001$ vs. 2 h) and MI model (D, $^{*}P < 0.05$ vs. 2 h) for 1 day. Arrows indicate the inject site of ^{18}F-FDG-labeled ADSC. A = anterior, P = posterior, RV = right ventricle, LV = left ventricle.

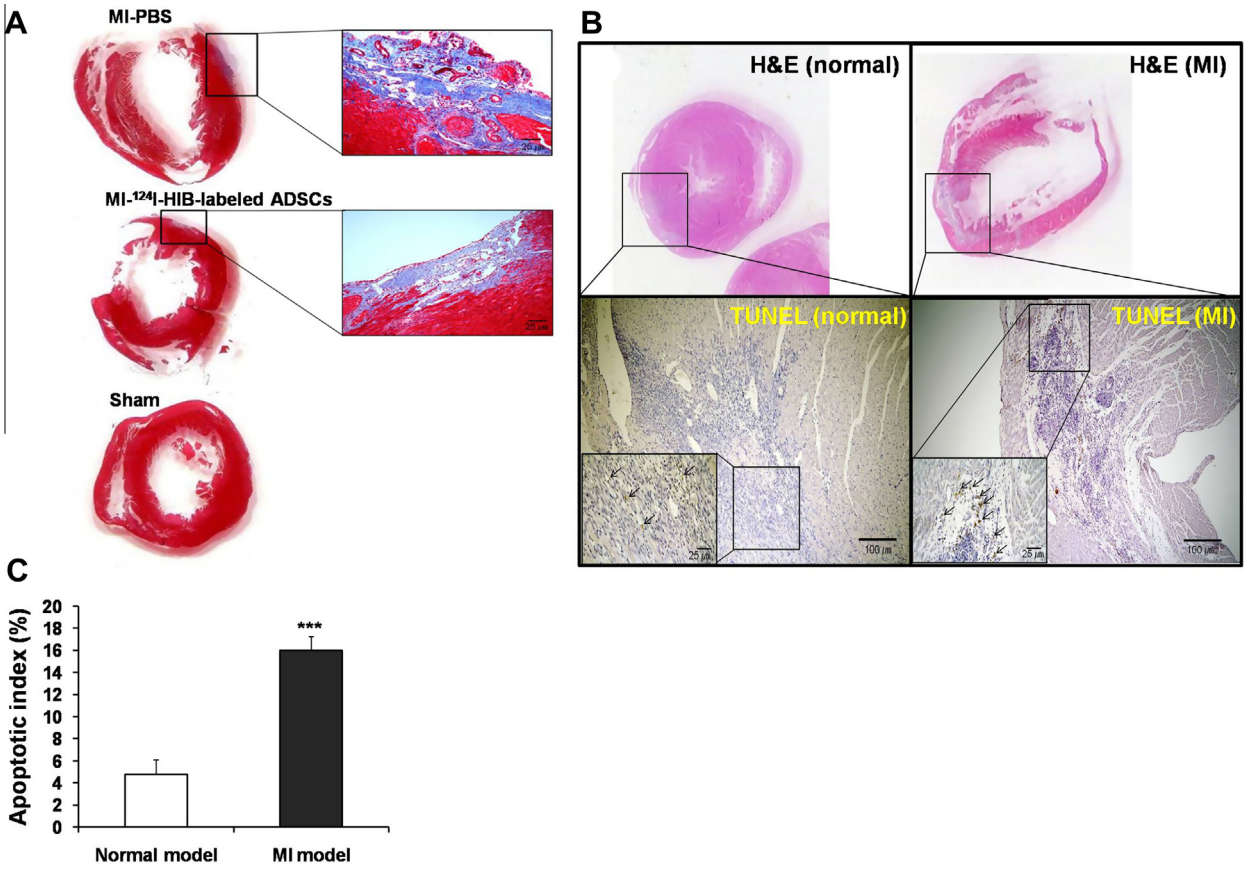

Fig. 4. Collagen deposition and apoptosis of transplanted ^{124}I-HIB-labeled ADSC in normal and MI model. (A) MT staining of myocardial tissue of PBS-injected, ^{124}I-HIB-labeled ADSCs transplanted, and sham-operated group. Each box represents higher magnification (×400) of images. (B) H&E and TUNEL staining (magnification ×100) of transplanted ^{124}I-HIB-labeled ADSC in normal and MI model. Arrows indicate TUNEL positive cells. (C) Apoptotic index of transplanted ^{124}I-HIB-labeled ADSC in normal (open bar) and MI model (solid bar) ($^{***}P < 0.0001$, normal vs. MI model).

3.4. In vivo imaging of transplanted ^{124}I-HIB-labeled ADSCs

In normal model, the transplanted ^{124}I-HIB-labeled ADSCs were monitored in the left myocardium until 9 days. In the normal model, radioactivity of the transplanted ^{124}I-HIB-labeled ADSCs at 9 days after transplantation remained at 24.67 ± 1.18% of the day 1 value (100%) ($P < 0.05$).

In MI model, monitoring of transplanted ^{124}I-HIB-labeled ADSCs was possible only until 3 days. In MI model, radioactivity of the transplanted ^{124}I-HIB-labeled ADSCs at 3 days after transplantation exhibited at 13.62 ± 7.66% of the 2 h value (100%) ($P < 0.05$). Twenty-one days after cell injection, dense staining of ^{124}I-HIB-labeling ADSCs deposits with hematoxylin was identified in the normal and MI model, at near the presumptive sites of ADSC injection, respectively (Fig. 2).

3.5. In vivo imaging of transplanted ^{18}F-FDG-labeled ADSCs

In the normal and MI model, the transplanted ^{18}F-FDG-labeled ADSCs were monitored until 2 h (Fig. 3A and B). After 1 day, radioactivity of ^{18}F-FDG-labeled ADSCs in the normal and MI model declined to below 1% of their initial injected dose (Fig. 3C and D).

3.6. Collagen deposition in the MI induced myocardium and apoptosis of transplanted ^{124}I-HIB-labeled ADSCs

In the group of PBS-injected or ^{124}I-HIB-labeled ADSC transplantation, the infarct area changed with fibrotic tissue and was densely stained with MT, but there was no MT staining-positive area in the sham-operated group (Fig. 4A).

TUNEL positive, apoptotic cells were detected in normal and MI model and transplanted ^{124}I-HIB-labeled ADSCs (Fig. 4B). In the transplanted ^{124}I-HIB-labeled ADSC area, the apoptotic index, the percentage of TUNEL-positive nuclei, were significantly higher in the MI (16 ± 1.22%) than in the normal model (4.8 ± 1.30%) ($P < 0.0001$) (Fig. 4C).

4. Discussion

We evaluated the ^{124}I-HIB as a direct labeling agent for in vivo survival monitoring of ADSCs in the normal and MI model, and therapeutic efficacy of ADSCs in MI.

^{124}I-HIB-labeled ADSCs, which were transplanted into normal and MI model, can be visualized via cell-associated radioactivity on PET/CT imaging. ^{124}I-HIB-labeled ADSCs clearly visualized the site of the transplanted ADSCs in the heart tissue (Fig. 2). ^{124}I-HIB-labeled ADSCs transplanted in normal model could be tracked for 9 days (Fig. 2), but that in MI model could be tracked for 3 days (Fig. 2). ADSC-like immature cells were detected in the presumptive cell injection site in normal and MI model (Fig. 2). Myocardial infarction influences the character of transplanted stem cells such as morbidity and mobility [19]. Penna et al. investigated the change of morphology and marker expression of mesenchymal stem cells (MSCs) implanted in isolated beating heart including normal and MI. They reported that morphological change and expression of differentiation marker GATA4 was observed in transplanted MSC in normal heart. Yet, MSCs in the infarcted hearts they maintain typical round shape, and form clusters of round-shaped cells in the border-zone of the infarcted area [19].

This difference reflects the poor viability of transplanted ADSCs in MI model due to harsh microenvironments in the infracted lesion [20]. Indeed, the percentage of apoptotic cell population in MI model transplanted ^{124}I-HIB-labeled ADSCs was higher compared to that in normal model at injection site (Fig. 4C). In the current study, visualization of transplanted ADSCs by PET imaging in MI was shorter than normal model, may reflect the harsh condition of MI.

Although the direct labeling method using ^{124}I-HIB cannot provide long-term imaging of viable cells as with reporter genes [21], it can provide the relatively more lasting cell survival rate of transplanted stem cells through a longitudinal quantitative image analysis than pre-established direct labeling agents with short half-lives such as ^{99m}Tc-hexamethylpropyleneamine oxime (^{99m}Tc-HMPAO) and ^{18}F-compound. Promising advantage of the current approach is the membrane inserting agent could be superior to ^{18}F-FDG or cell penetrating agent. ^{18}F-FDG uptake might be dependent on cellular characteristic including glucose transporter and hexokinase expression level. In general, ^{18}F-FDG can be highly uptake in cancer cell rather than non-proliferating cells including stem cell [22]. Penetrating agent such as ^{99m}Tc-HMPAO and ^{111}In-oxine can be trapped in cell and easily released from cell [23,24]. Direct labeling agents for stem cell monitoring must have a high level of cell labeling efficiency, be non-toxic to target cells, and produce no adverse effects for stem cell differentiation. To provide the safety of ^{124}I-HIB as a labeling agent, we checked ADSC viability after ^{124}I-HIB labeling. ^{124}I-HIB labeled ADSC was nearly 100% viable state up to 144 h, and stable in vitro for 24 h. In this study, ADSC labeling efficiency with ^{124}I-HIB was superior to that of ^{18}F-FDG at same labeling condition and also higher than that of hexadecyl-4-^{18}F-fluorobenzoate (^{18}F-HFB) as anchoring to cell membrane in which labeling yield is 25% using rat mesenchymal stem cell previously reported [25]. To make sure of maintenance of ADSC characteristic as progenitor cell after ^{124}I-HIB labeling, we checked differentiation potential of ^{124}I-HIB-labeled ADSCs. ^{124}I-HIB-labeled ADSC could differentiate into osteo-, chondro-, adipo- and cardiomyogenic lineage (Fig. 1F and G). This result suggests that radiolabeling of ADSCs using ^{124}I-HIB did not compromise stem cell differentiation potential of stem cells. Therefore, these results strongly provide that stem cell labeling with ^{124}I-HIB was a safe and appropriate method to monitor transplanted stem cells due to no adverse effect to ADSC characteristic as progenitor cell. However, ^{124}I-HIB has no gene product compared to that of reporter gene imaging, so it is free from immunogenic problems. Thus, ^{124}I-HIB is free from previously noted obstacles in clinical trials [26].

This is the first report for monitoring the behavior change of stem cells in normal and ischemic conditions using a direct labeling agent, ^{124}I-HIB-based radionuclide via PET imaging. Stem cell labeling with ^{124}I-HIB was a safe, simple, and appropriate method to monitor transplanted stem cells. This method provided relatively long-term monitoring after cell transplantation, and reflects stem cell behavior in ischemic conditions due to its long half-life. Therefore, this novel approach may provide new insights on the roles of stem cell monitoring in living bodies for stem cell therapy from pre-clinical studies to clinical trials.

Acknowledgments

This work was funded by the Nuclear R&D (Grant Codes: 20090081817, 20120006386 and 2012013480) and BAERI (Grant Code: 20090078235) Programs of NRF, funded by MEST – Republic of Korea.

Appendix A. Supplementary data

Supplementary data associated with this article can be found, in the online version, at http://dx.doi.org/10.1016/j.bbrc.2014.11.019.

References

[1] E. Falk, P.K. Shah, V. Fuster, Coronary plaque disruption, Circulation 92 (1995) 657–671.

[2] Y. Tang, X. Gan, R. Cheheltani, E. Curran, G. Lamberti, B. Krynska, M.F. Kiani, B. Wang, Targeted delivery of vascular endothelial growth factor improves stem cell therapy in a rat myocardial infarction model, Nanomedicine 10 (2014) 1711–1718.
[3] K. Dickstein, J. Bebchuk, J. Wittes, The high-risk myocardial infarction database initiative, Prog. Cardiovasc. Dis. 54 (2012) 362–366.
[4] M. Al-Nbaheen, R. Vishnubalaji, D. Ali, A. Bouslimi, F. Al-Jassir, M. Megges, A. Prigione, J. Adjaye, M. Kassem, A. Aldahmash, Human stromal (mesenchymal) stem cells from bone marrow, adipose tissue and skin exhibit differences in molecular phenotype and differentiation potential, Stem Cell Rev. 9 (2013) 32–43.
[5] P. De Coppi, G. Bartsch Jr., M.M. Siddiqui, T. Xu, C.C. Santos, L. Perin, G. Mostoslavsky, A.C. Serre, E.Y. Snyder, J.J. Yoo, M.E. Furth, S. Soker, A. Atala, Isolation of amniotic stem cell lines with potential for therapy, Nat. Biotechnol. 25 (2007) 100–106.
[6] S. Gronthos, J. Brahim, W. Li, L.W. Fisher, N. Cherman, A. Boyde, P. DenBesten, P.G. Robey, S. Shi, Stem cell properties of human dental pulp stem cells, J. Dent. Res. 81 (2002) 531–535.
[7] Y. Jiang, B.N. Jahagirdar, R.L. Reinhardt, R.E. Schwartz, C.D. Keene, X.R. Ortiz-Gonzalez, M. Reyes, T. Lenvik, T. Lund, M. Blackstad, J. Du, S. Aldrich, A. Lisberg, W.C. Low, D.A. Largaespada, C.M. Verfaillie, Pluripotency of mesenchymal stem cells derived from adult marrow, Nature 418 (2002) 41–49.
[8] M.F. Pittenger, A.M. Mackay, S.C. Beck, R.K. Jaiswal, R. Douglas, J.D. Mosca, M.A. Moorman, D.W. Simonetti, S. Craig, D.R. Marshak, Multilineage potential of adult human mesenchymal stem cells, Science 284 (1999) 143–147.
[9] F. Lin, Adipose tissue-derived mesenchymal stem cells: a fat chance of curing kidney disease?, Kidney Int 82 (2012) 731–733.
[10] N. Yamamoto, H. Akamatsu, S. Hasegawa, T. Yamada, S. Nakata, M. Ohkuma, E. Miyachi, T. Marunouchi, K. Matsunaga, Isolation of multipotent stem cells from mouse adipose tissue, J. Dermatol. Sci. 48 (2007) 43–52.
[11] F.M. Bengel, V. Schachinger, S. Dimmeler, Cell-based therapies and imaging in cardiology, Eur. J. Nucl. Med. Mol. Imaging 32 (2005) S404–S416.
[12] A.M. Mozid, S. Arnous, E.C. Sammut, A. Mathur, Stem cell therapy for heart diseases, Br. Med. Bull. 98 (2011) 143–159.
[13] V. Russo, S. Young, A. Hamilton, B.G. Amsden, L.E. Flynn, Mesenchymal stem cell delivery strategies to promote cardiac regeneration following ischemic injury, Biomaterials 35 (2014) 3956–3974.
[14] Z.Q. Li, M. Zhang, Y.Z. Jing, W.W. Zhang, Y. Liu, L.J. Cui, L. Yuan, X.Z. Liu, X. Yu, T.S. Hu, The clinical study of autologous peripheral blood stem cell transplantation by intracoronary infusion in patients with acute myocardial infarction (AMI), Int. J. Cardiol. 115 (2007) 52–56.
[15] D. Orlic, J. Kajstura, S. Chimenti, D.M. Bodine, A. Leri, P. Anversa, Bone marrow stem cells regenerate infarcted myocardium, Pediatr. Transpl. 7 (2003) 86–88.
[16] T.C. Hung, Y. Suzuki, T. Urashima, A. Caffarelli, G. Hoyt, A.Y. Sheikh, A.C. Yeung, I. Weissman, R.C. Robbins, J.W. Bulte, P.C. Yang, Multimodality evaluation of the viability of stem cells delivered into different zones of myocardial infarction, Circ. Cardiovasc. Imaging 1 (2008) 6–13.
[17] Y. Zhang, M. Ruel, R.S. Beanlands, R.A. deKemp, E.J. Suuronen, J.N. DaSilva, Tracking stem cell therapy in the myocardium: applications of positron emission tomography, Curr. Pharm. Des. 14 (2008) 3835–3853.
[18] P.H. Carvalho, A.P. Daibert, B.S. Monteiro, B.S. Okano, J.L. Carvalho, D.N. Cunha, L.S. Favarato, V.G. Pereira, L.E. Augusto, R.J. Del Carlo, Differentiation of adipose tissue-derived mesenchymal stem cells into cardiomyocytes, Arq. Bras. Cardiol. 100 (2013) 82–89.
[19] C. Penna, S. Raimondo, G. Ronchi, R. Rastaldo, D. Mancardi, S. Cappello, G. Losano, S. Geuna, P. Pagliaro, Early homing of adult mesenchymal stem cells in normal and infarcted isolated beating hearts, J. Cell. Mol. Med. 12 (2008) 507–521.
[20] H. Haider, M. Ashraf, Preconditioning and stem cell survival, J. Cardiovasc. Transl. Res. 3 (2010) 89–102.
[21] M. Rodriguez-Porcel, O. Gheysens, I.Y. Chen, J.C. Wu, S.S. Gambhir, Image-guided cardiac cell delivery using high-resolution small-animal ultrasound, Mol. Ther. 12 (2005) 1142–1147.
[22] C. Plathow, W.A. Weber, Tumor cell metabolism imaging, J. Nucl. Med. 49 (2008) 43S–63S.
[23] I.Y. Chen, J.C. Wu, Cardiovascular molecular imaging: focus on clinical translation, Circulation 123 (2011) 425–443.
[24] A.M. Peters, H.J. Danpure, S. Osman, R.J. Hawker, B.L. Henderson, H.J. Hodgson, J.D. Kelly, R.D. Neirinckx, J.P. Lavender, Clinical experience with ^{99m}Tc-hexamethylpropylene-amineoxime for labelling leucocytes and imaging inflammation, Lancet 2 (1986) 946–949.
[25] B. Ma, K.D. Hankenson, J.E. Dennis, A.I. Caplan, S.A. Goldstein, M.R. Kilbourn, A simple method for stem cell labeling with fluorine 18, Nucl. Med. Biol. 32 (2005) 701–705.
[26] J.V. Terrovitis, R.R. Smith, E. Marban, Assessment and optimization of cell engraftment after transplantation into the heart, Circ. Res. 106 (2010) 479–494.